Received: 3 October 2021 | Revised: 9 November 2021 | Accepted: 13 November 2021

DOI: 10.1002/agt2.148

Aggregate WILEY

REVIEW

Endowing inorganic nanomaterials with circularly polarized luminescence

Dongxue Han[1] | **Chengxi Li**[1,3] | **Chengyu Jiang**[1,3] | **Xue Jin**[1] | **Xiongbin Wang**[2,4] | **Rui Chen**[4] | **Jiaji Cheng**[2] | **Pengfei Duan**[1,3]

[1] CAS Key Laboratory of Nanosystem and Hierarchical Fabrication, CAS Center for Excellence in Nanoscience, National Center for Nanoscience and Technology, Beijing, P. R. China

[2] Key Laboratory for the Green Preparation and Application of Functional Materials, Ministry of Education, School of Materials Science and Engineering, Hubei University, Wuhan, P. R. China

[3] University of Chinese Academy of Sciences, Beijing, P. R. China

[4] Department of Electrical and Electronic Engineering, Southern University of Science and Technology, Shenzhen, P. R. China

Correspondence
Jiaji Cheng, Key Laboratory for the Green Preparation and Application of Functional Materials, Ministry of Education, School of Materials Science and Engineering, Hubei University, Wuhan, 430062, P. R. China.
Email: jiajicheng@hubu.edu.cn
Pengfei Duan, CAS Key Laboratory of Nanosystem and Hierarchical Fabrication, CAS Center for Excellence in Nanoscience, National Center for Nanoscience and Technology, No. 11 ZhongGuanCun BeiYiTiao, Beijing 100190, P. R. China.
Email: duanpf@nanoctr.cn

Funding information
National Natural Science Foundation of China, Grant/Award Numbers: 21773103, 21802027, 91856115; Strategic Priority Research Program of the Chinese Academy of Sciences, Grant/Award Number: XDB36000000; Ministry of Science and Technology of the People's Republic of China, Grant/Award Number: 2017YFA0206600

Abstract

Recently, materials with circularly polarized luminescence (CPL) properties have attracted substantial attention because they offer new perspectives in fundamental research and wide applications in photonics, bio-encoding, catalysis, and so forth. Such importance has recently promoted the development of CPL-active materials from the traditional realm of organics to newly released areas in inorganics. Due to the advantages of inorganic nanomaterials in stability, high luminescent quantum efficiency, material diversity, and the diversity of shapes and sizes, extensive research about CPL active inorganic nanomaterials has been done in the past decades leading to great signs of progress on synthesis, characterizations, and potential applications. In this review, therefore, we will thoroughly describe the general design principles of inorganic nanomaterials with CPL activity, basically according to the origins of chirality in inorganic nanomaterials: intrinsic chirality in inorganic nanomaterials, ligand-induced chirality, and structural chirality caused by the supramolecular assembly, respectively. The representative applications of the CPL-active inorganic nanomaterials are presented with respect to challenges, prospective, and problems that unsolved to date.

KEYWORDS

circularly polarized luminescence, inorganic nanomaterials, perovskite nanocrystal, quantum dot, upconversion nanoparticle

1 | INTRODUCTION

Chirality is a remarkable natural attribute, which refers to a geometrical concept describing an object that is non-superimposable on its mirror image.[1] As a unique feature of a matter's symmetry, it occurs at all length scales from subatomic particles to molecules, then to micro-scale, life systems, and even to galaxies. The amazing phenomenon of chirality has stimulated scientists in extensive research fields from photonics to biochemistry,[2] medicine,[3] and catalysis.[4] Among the characteristics of chiral materials, optical activity, including absorption and emission, gradually absorbs scientists' attention.[5] The absorption of chiral materials could be detected by circular dichroism (CD) instrument, which presents ground state chiral information.[6] While the emission of chiral materials can be confirmed by circularly polarized luminescence (CPL) measurement, which clarifies conformational and structural information associated with optically active materials in the excited state.[7] Such chiroptical phenomena have been proved to be effective probes for chiral nanostructures and give imperative help to the following research.

In fact, optically active luminescent materials with CPL property have exhibited great potentials in three-dimensional displays,[8–10] optical data storage,[11] and optical sensors.[12,13] These versatile functionalities bring in the rapid growth of the CPL-active inorganic nanostructures, with intermediate sizes between molecules of Angstrom and objects of micrometers, providing opportunities to control the chirality of light and the reactions of asymmetry synthesis.[14–18] The discovery of CPL in inorganic nanostructures including chiral II–VI group semiconductor nanostructures,[19,20] perovskites,[21,22] transition metal dichalcogenides,[23,24] metal nanocrystal,[25] and so on, stimulated the fast development of fundamental and using investigation in biology, chemistry, physics, and medicine.[26] The fascinating chiral nanostructures and luminescence characteristics of CPL-active inorganic nanomaterials motivate researchers to explore their properties for exhibiting intensifying chiroptical activity. In general, the origination of chirality can be obtained from three possible mechanisms: 1) intrinsic chirality formed by chiral nanostructures as the existence of the chiral defects result in the reduced symmetry,[27] 2) ligand-induced chirality in inorganic nanostructures such as metal clusters, metal nanocrystals (NCs), quantum dots (QDs), carbon-based materials and semiconductors. This chirality closely relates to the morphology, size, and surface chemistry of the nanostructures,[28] 3) chirality transfer through chiral self-assembled nanostructures of achiral inorganic materials.[29,30] These three mechanisms are widely explored by investigators to construct chiral inorganic nanomaterials with CPL activity.

Pursuing a large circular polarization is still a big challenge in the realm of CPL-active materials. Compared with chiral organic compounds, the CPL activity of chiral inorganic materials is affected by two main factors: the size of the object and the degree of asymmetry. Thus, the merits of CPL-active inorganic nanomaterials over organic materials incorporate the capability of controlling their properties during the synthetic process, as well as the possibility to achieve significantly higher emission efficiencies and luminescence dissymmetry factors. In practice, there are many critical reviews that specifically introduced chiral inorganic nanomaterials, but most of them focused on the optical activity at the ground state.[31–35] Comprehensive classification and summary of chirality at the excited state of inorganic nanomaterials are rarely mentioned. Understanding the relationship between chiral inorganic nanostructures and circularly polarized light will enrich the optical properties of these chiral nanomaterials and broaden the scope of their applications. In addition, an in-depth investigation of CPL-active inorganic nanomaterials would help us to understand the origin of homochirality on the earth, which is often connected with cosmic circularly polarized light.

As an ever-developing research field, it is necessary to thoroughly understand the influencing factors about the optical activity of CPL-active inorganic nanomaterials. Herein, we emphasize the recent progress of CPL-active inorganic nanomaterials and the g_{lum} of chiral inorganic systems derived from the aforementioned three possible mechanisms (Table 1). The materials synthesis methods, design principles as well as the origination of the chirality are discussed. We also give remaining challenges and perspectives for future investigation in this field, concerning both the ongoing basic research and promising applications, which might provide timely insights for researchers to design CPL-active inorganic nanomaterials with high dissymmetric factors.

2 | BASIC UNDERSTANDING OF CD AND CPL PHENOMENA

Circular dichroism (CD) is a form of absorption spectroscopy that is one of the most widely used techniques for investigating the chiroptical properties of materials. CD is defined as the absorption difference of circularly polarized light with different handedness which could be expressed as follows:

$$CD = \Delta A = A_L - A_R$$

where the observed absorption following left- and right-hand circular polarized light is denoted as A_L and A_R, respectively. To exclude the influence of sample concentration and light path length, dissymmetry factor is often used which is defined as follows:

$$g_{abs} = \frac{2(A_L - A_R)}{A_L + A_R} = \frac{\Delta A}{A}$$

where A is the absorbance of equivalently average of A_L and A_R. The dissymmetry is often referred to as anisotropic factor or simply g-factor.[36]

As for CPL spectroscopy, it measures the differences of spontaneous emission intensity of left- (I_L) and right-hand (I_R) circular polarized radiation of a sample after photoexcitation with non-polarized light, which could be regarded as an analog of CD spectroscopy, and could be expressed as follows[7]:

$$\Delta I = I_L - I_R$$

Similarly, the luminescence dissymmetry factor (g_{lum}) is defined for evaluating the degree of circularly polarized radiation, which is similar to the anisotropic factor, and could be indicated as follows[37]:

$$g_{lum} = \frac{2(I_L - I_R)}{I_L + I_R} = \frac{\Delta I}{I}$$

Here, I is the mean value of the summation of I_L and I_R. Obviously, g_{lum} is a scalar quantity without any units ranging from +2 to –2, which is corresponding to the total left and right-hand CPL of samples, respectively. The samples would also show no CPL signal when the dissymmetry factor is zero. Recently, Arrico et al., proposed a useful metric for evaluating the quantity of CPL based on traditional employed metrics of fluorescence brightness (B) which is known as the product of emission quantum yield (φ) and molar extinction coefficient (ε_{abs})[38]:

$$B = \varphi \times \varepsilon_{abs}$$

The brightness (B_{CPL}) for CPL is defined as follows:

$$B_{CPL} = \varphi \times \varepsilon_{abs} \times \frac{|g_{lum}|}{2}$$

TABLE 1 The reported g_{lum} for CPL-active inorganic nanomaterials

Chirality origination mechanism	Chiral inorganic nanomaterials	$\|g_{lum}\|$	Reference
Intrinsic chirality	CdS@ferritin	$\sim 3.5 \times 10^{-4}$	[44]
	(*R*-/*S*-MBA)$_2$PbI$_4$	~0.05	[47]
	R-/*S*-MnBr$_3$	$\sim 6.1 \times 10^{-3}$	[48]
	TbPO$_4$·H$_2$O NCs	~0.4	[49]
Ligand-induced chirality	CdSe QDs	$\sim 3.0 \times 10^{-3}$	[54]
	CdSe/CdS DRs	$\sim 3.9 \times 10^{-4}$	[55]
	CdSe/CdS NCs	$\sim 8.5 \times 10^{-4}$	[56]
	CsPbBr$_3$ NCs	$\sim 7.0 \times 10^{-3}$	[57]
	FAPbBr$_3$ NCs	$\sim 6.8 \times 10^{-2}$	[58]
Chiral-assembly	Nanobamboo/QDs	~0.01	[64]
	CsPbBr$_3$ NCs	$\sim 6.0 \times 10^{-3}$	[65]
	TCPP@SiO2	$\sim 5.0 \times 10^{-3}$	[66]
	Spirocyclic silver cluster	0.16	[67]
	R/*S*-Cu$_2$I$_2$(BINAP)$_2$	$\sim 9.5 \times 10^{-3}$	[68]
	L/D-AuNCs	$\sim 3.6 \times 10^{-3}$	[69]
	L-/D-GAm QDs	$\sim 4.4 \times 10^{-3}$	[70]
	L-/D-GAm CsPbX$_3$	$\sim 7.3 \times 10^{-3}$	[71]
	BTABA/UCNPs	$\sim 1.2 \times 10^{-2}$	[72]
	N*LCs/PKNCs	~1.1	[75]
	CNCs/QRs	~0.45	[81]
	CNCs/QDs	~0.48	[82]

The definition of CPL brightness is very useful for comparing and evaluating the performances of different circular polarized emitters.

In quantum chemistry, transition probability could be used for describing the relationship of ΔI and I to properties of molecules. For a given transition of initial emitting state i to a final state j, the differential emission intensity could be estimated as follows[5]:

$$\Delta I(\lambda)_{ij} = \frac{hc}{2\pi\lambda}\left(P_{ij}^{L} - P_{ij}^{R}\right) N_n G_\delta(\lambda) = \frac{hc}{2\pi\lambda}\Delta P_{ij} N_n G_\delta(\lambda)$$

where P_{ij}^{L} and P_{ij}^{R} are transition probability of emitting a left and right circularly polarized photon, respectively. N_n is the carrier population on the initial emitting state. $G_\delta(\lambda)$ is the lineshape function. It needs to be mentioned that time and orientation dependence of carrier population and lineshape function are not considered for simplicity. More specifically, in the Cartesian coordinate system (x y z), we assume that the emitted light is detected along the z-axis. Then, the differential transition probability could be expressed as follows:

$$\Delta P_{ij} = P_{ij}^{L} - P_{ij}^{R} = -K(\lambda^3)\left[4i\left(\mu_x^{ij} m_x^{ij} + \mu_y^{ij} m_y^{ij}\right)\right]$$

where μ^{ij} and m^{ij} are electric and magnetic transition dipole moments, respectively. It could be seen that the probability is nonzero when the molecule's electric and magnetic transition dipole moments are nonzero. The as mentioned equation is only true for chiral molecules in the absence of external fields. Besides, the total transition probability could be calculated as:

$$P_{ij} = P_{ij}^{L} + P_{ij}^{R} = 2K(\lambda^3)\left[\left|\mu_x^{ij}\right|^2 + \left|m_x^{ij}\right|^2 + \left|\mu_y^{ij}\right|^2 + \left|m_y^{ij}\right|^2\right]$$

We assume that the number of emitted molecules is not related to the orientation and that lineshape and total emission are identical. Then, the luminescence dissymmetry factor could be expressed as follows:

$$g_{lum} = \frac{\Delta I}{I} = \frac{\Delta P_{ij}}{P_{ij}/2} = -4i\frac{\mu_x^{ij} m_x^{ij} + \mu_y^{ij} m_y^{ij}}{\left|\mu_x^{ij}\right|^2 + \left|m_x^{ij}\right|^2 + \left|\mu_y^{ij}\right|^2 + \left|m_y^{ij}\right|^2}$$

Further, for molecules with random distribution, the more general luminescence dissymmetry factor could be expressed using a simple equation[37]:

$$g_{lum} = 4\mathrm{Re}\left[\frac{\vec{\mu}_{ij}\cdot\vec{m}_{ij}}{\left|\vec{\mu}_{ij}\right|^2 + \left|\vec{m}_{ij}\right|^2}\right]$$

Based on the above equation, we could figure out that larger anisotropy/dissymmetry factors are obtained when both the electric and magnetic transitions are inherently weak. One may also obtain a high dissymmetry factor when the transition is magnetic dipole allowed and the electric dipole is forbidden. For electric dipole allowed transition, the equation is dominated by the reciprocal of electric transition dipole moment.

Commercialized CD instruments have been available for several decades while most instruments for CPL measurement are homemade in which limits the development of CPL spectroscopy. Recently, commercial CPL has become available. The basic idea for a CPL measurement set-up is to convert the CPL into linear polarization in which differences in measuring the intensity of the modulated linear polarized light in phase are proportional to the CPL. Generally, the total luminescence that we observe from the sample after excitation is elliptical where CPL has only a very small fraction among it. Hence, special care should be taken for avoiding the occurrent of false signals and obtain true CPL signals. The linear polarized emission light is one of the most relevant artifactual sources for obtaining true CPL. Photoelastic modulator is a key optical component that is not perfect which has a very weak birefringence effect, and the linear polarized emission light would transform into CPL resulting in a pseudo signal. Another artifact related to linear polarization that would contribute to the recorded signal comes from the photoselection effect which could be understood that the polarization and direction of excitation light, as well as the absorption dipole, would directly influence the orientational distribution of the excited molecules in which the CPL is very difficult to be measured with the presence of linear polarized component.[39,40] A further artifact that should be considered would often present when the CD and CPL bands are partially overlapped. In this situation, the emitting left-hand and right-hand CPL of the sample would be absorbed by itself differently before being recorded by the detector.

3 | CPL IN CHIRAL INORGANIC NANOMATERIALS

In recent years, the research of chiral inorganic nanomaterials with CPL property has been tremendously expanded. How to ingeniously introduce chirality is a big challenge in constructing CPL-active inorganic nanomaterials. Therefore, in order to fabricate chiral inorganic nanostructures, various methods have been employed. The preparation of pure nanostructures possessing intrinsic chirality is quite difficult. Modifying chiral ligands on the surface of the nanostructures through the ligand exchange approach and incorporating inorganic nanomaterials into a confined chiral environment by supramolecular self-assembly had been verified to be effective methods for the fabrication of CPL-active inorganic nanomaterials. In this section, three categories based on different chirality origination mechanisms: intrinsic chirality, ligand-induced chirality, and chiral-assembly will be introduced (Figure 1) for the preparation of chiral inorganic nanomaterials with CPL property.

3.1 | CPL in inorganic nanomaterials with intrinsic chirality

Generally, the intrinsic chirality in inorganic nanomaterials is major formed by chiral crystals, lattice distortions, and defects. The intrinsically chiral NCs are generally divided into two different types: 1. chiral shape like helix or "twisted" construction; 2. chiral lattice, such as the chiral configuration of the building blocks.[41–43] Semiconductor QDs as inorganic nanomaterials derived from the quantum confinement effect have attracted much attention because of their optically adjustable light emissions. However, most of the QDs were prepared with chiral stabilizers, while the chiral stabilizers only distorted the QDs surface and cannot transmit an enantiomeric structure to the QDs core. It is still a big challenge to achieve a CPL signal from the chiral crystal structure in terms of these kinds of QDs. Later, Yamashita and co-workers have demonstrated that surface trapping sites and direct transition did a favor to the impressive left-handed CPL emissions of cadmium sulfur (CdS) QDs made in ferritin.[44] Briefly, the horse spleen ferritin acted as the hollow chiral template to prepare QDs into chiral nanostructures with CPL activity. The CPL of CdS@ferritin exhibited a peak at 498 nm and broadband at 780 nm, which should be derived from the direct transition band and surface-trapping sites, respectively. The reason for this phenomenon is that the chiral configurations of the chelating amino acid residues were transmitted to the QDs crystal lattice during anisotropic crystal formation. After laser photo etching, the CPL bands derived from surface-trapping sites showed obvious blue-shift as the size of QDs decreased, whereas the band from the direct transition disappeared.

Similar to the QDs, halide perovskites have also been a hot topic of research due to their excellent performances in multiple applications, including light-emitting diodes and solar cells. The chiral semiconducting perovskites with the CPL property were a promising candidate for developing circularly polarized light sources.[45,46] Chiral perovskites related to CPL emission have been demonstrated in many reports. Nevertheless, it is still a challenge to obtain CPL from chiral perovskite based on intrinsic chirality. For example, Li and co-workers successfully synthesized CPL-active pure chiral (*R*-/*S*-MBA)$_2$PbI$_4$ (MBA = $C_6H_5C_2H_4NH_3$) two-dimensional (2D) perovskites with needle shape and size in millimeter, as shown in Figure 2A.[47] ·The chiral 2D perovskites were synthesized by using S-MBA and R-MBA as chiral ligands through a solution approach, and the resulting crystal had an orange color and needle-like shape with millimeter size. Furthermore, at 77 K, the polarization-sensitive photoluminescence investigations of (R-/S-MBA)2PbI4 microplates revealed a clear intensity difference between the left-handed (σ^-) and right-handed (σ^+) CPL centered about 505 nm for the chiral (R-MBA)$_2$PbI$_4$ and (S-MBA)$_2$PbI$_4$ microplates. The temperature-dependent polarization-sensitive photoluminescence investigation was also performed from 77 to 290 K. As a result, the CPL degree continuously decreased, indicating that the chiral molecules induced lattice distortion is possible the major reason for the generation of chirality. Similarly, this method can be employed to endow perovskite ferroelectric materials with CPL activity. The organic-inorganic perovskite enantiomorphic ferroelectrics, (*R*)- and (*S*)-3-(fluoropyrrolidinium)MnBr$_3$ (*R*-/*S*-MnBr$_3$) with CPL activity were reported by the Fu and co-workers.[48] The structures of perovskite composed infinite chains, forming by (*R*)- and (*S*)-3-fluoropyrrolidinium cations, face-sharing MnBr$_6$ octahedra, and spacing these chains, as shown in Figure 2B. In addition, the *R*- and *S*-MnBr$_3$ display mirror-image CPL signal from 550 to 700 nm, and the g_{lum} was around $\pm 6.1 \times 10^{-3}$. It may be caused by the existence of chiral cations

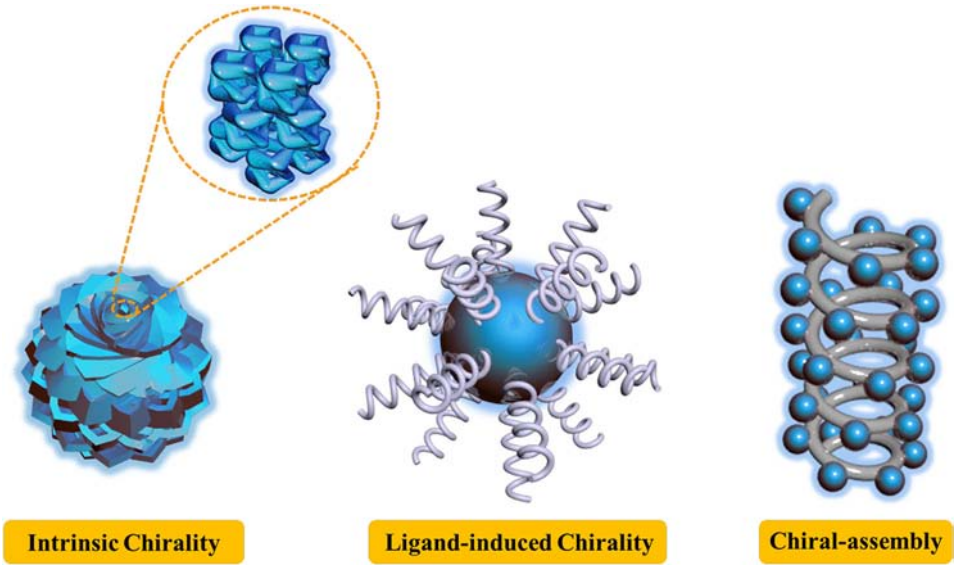

FIGURE 1 Inorganic nanostructures with CPL activity: intrinsic chirality, ligand-induced chirality, and chiral-assembly

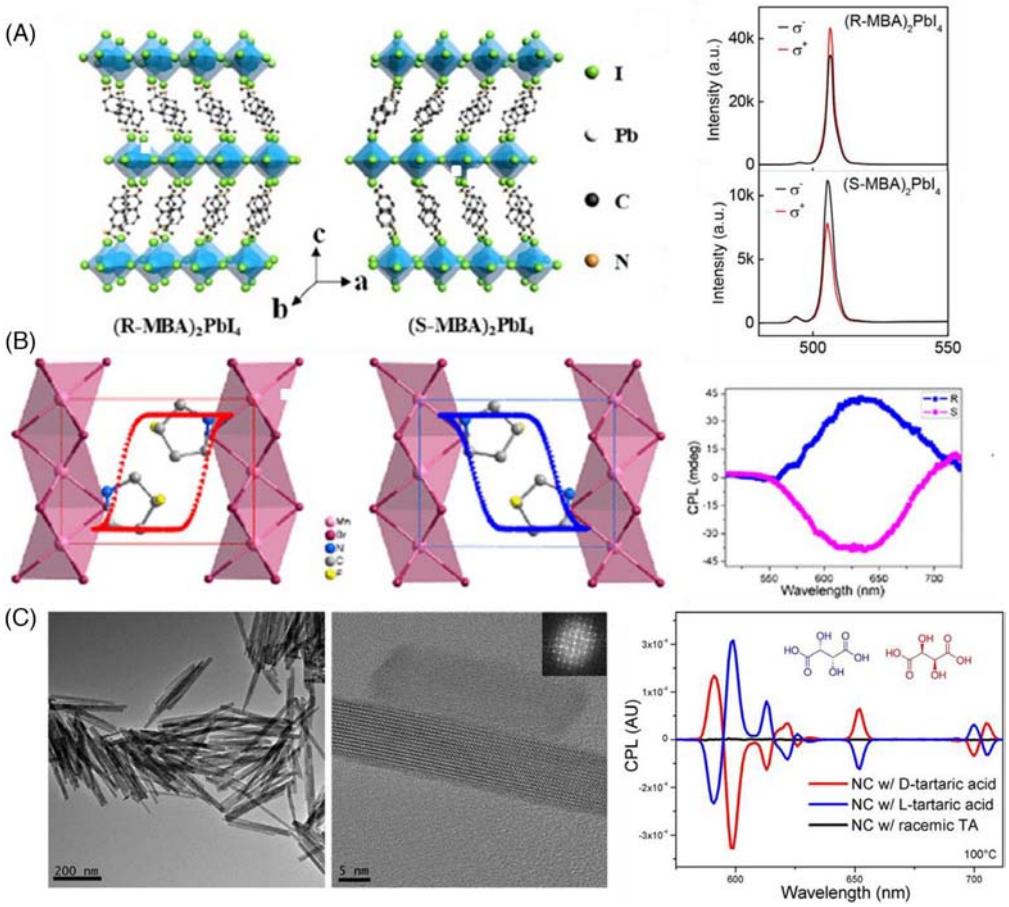

FIGURE 2 Intrinsic-chirality-based circularly polarized luminescence (CPL)-active inorganic nanomaterials. (A) Left: The characterization and crystal structure of pure chiral two-dimensional (2D) perovskites (*R*-/*S*-MBA)$_2$PbI$_4$; Right: CPL spectra of (*R*-MBA)$_2$PbI$_4$; CPL spectra of (*S*-MBA)$_2$PbI$_4$; excited by a 473 nm laser at 77 K. Reproduced with permission: Copyright 2019, American Chemical Society.[47] (B) The structure (left), CPL spectra (right) of Perovskite Ferroelectrics *S*-/*R*-MnBr$_3$. Reproduced with permission: Copyright 2020, American Chemical Society.[48] (C) Left: transmission electron microscopy (TEM) images of the synthesized Eu^{3+}-doped $TbPO_4{\cdot}H_2O$ NCs; Right: CPL spectra of chiral $TbPO_4{\cdot}H_2O$ NCs. Reproduced with permission: Copyright 2019, National Academy of Sciences[49]

that CPL activity of the enantiomers regulated by the spatial configuration of the octahedral Mn^{2+}. These works provide a general method for constructing intrinsic-chirality-based inorganic-organic perovskite nanomaterials with CPL activity.

Besides QDs and perovskite, the chiral NCs with intrinsic chirality composed of various chiral inorganic compounds have emerged. For example, Markovich and co-workers reported the CPL emission from intrinsically chiral lanthanide phosphate NCs.[49] In this work, chiral Eu^{3+}-doped

$TbPO_4{\cdot}H_2O$ rod-shaped NCs were prepared and the transmission electron microscopy (TEM) of single crystals (SCs) structure was shown in Figure 2C. During the crystal formation procedure, chiral tartaric acid (D-/L-TA), coordinating with the lanthanide cations via its carboxylate groups, determined the nanocrystal handedness through left- and right-handed excess by a discontinuous transition. Resulting in that NCs displaying spontaneous symmetry breaking and emitting strong circularly polarized light. $TbPO_4{\cdot}H_2O$ NCs synthesized in the presence of L-TA or D-TA display right-hand or left-hand CPL, respectively, and the g_{lum} value reached ~0.4, which is about to the highest values of the enantiomerically pure chiral lanthanide complex. This work provides a novel strategy for the enantioselective synthesis of intrinsically chiral inorganic crystals with CPL property.

In addition, Gun'ko and co-workers reported that the intrinsic chirality of ZnS coated CdSe QDs and quantum rods (QRs) was shown after stabilizing by achiral ligands. A suitable chiral ligand and a conventional phase transfer method are able to make these inherently chiral semiconducting NCs selectively separated.[50] The separation of the enantiomers of CdSe/ZnS NCs dissolved in chloroform could be achieved by the method of adding a concentrated methanol solution of D- or L-cysteine while stirring them in the presence of distilled water. Except for CdSe/ZnS, many other quantum nanostructures, for example, CdS nanotetrapods and QRs, could be separated in this method, which will blaze new and exciting paths in the separation and research of CPL-active semiconductor nanomaterials. Zhu and co-workers successfully discovered optically active chiral $CsPbBr_3$ inorganic perovskite nanostructures, which exhibited a controllable and temperature-dependent CD via employing artificial intelligence of things technology, synthesis, characterization, and parameter optimization in cloud lab.[51] This method facilitates the identification of CPL-active novel materials by providing not only insights into the chiral genesis of NCs, but also multidisciplinary linkages between chemistry and IT technologies.

3.2 | Chiral capping reagent-induced CPL

Ligand-induced chirality in inorganic nanomaterials with CPL property has the potential to be applied in chiral biosensors, enantioselective synthesis, and chiroptical devices due to their excellent physicochemical properties, such as chemical stability, surface functionality, and adjustable quantum confinement effects.[52,53] Chiroptical response in CPL spectra can be originated from chiral interactions between chiral capping reagent and achiral core, ligand-induced chiral defects or surfaces. In the terms of chiral interactions, orbital coupling and Coulombic interaction are regarded as the dominating mechanisms for chirality transfer. In 2013, Balaz and co-workers first reported the ligand-induced CPL in QDs.[54] The D- and L-cysteine-capped cadmium selenium (CdSe) QDs were prepared from achiral oleic acid capped CdSe by the method of post-synthetic ligand exchange, resulting in displaying size-dependent right-handed CPL and left-handed CPL, respectively. The origin of the obtained chirality was associated with the hybridization of a chiral ligand with the highest occupied orbitals of CdSe molecular. The optimized design of CPL-active QDs with adjustable chiroptical properties will probably lead to potential applications in chiroptical inorganic nanomaterials.

Cheng et al. successfully prepared D- and L-cysteine-capped CdSe-dot/CdS-rods (DRs) with tunable CPL behaviors with a maximum g_{lum} value (4.66×10^{-4}) as shown in Figure 3A.[55] In this work, firstly, the CdSe/CdS DRs were obtained in the organic phase. Then the reactional products reacted with D-/L-cysteine through the process of ligand-exchanged in the aqueous phase. The geometry-dependent CD and CPL phenomena were also measured. Their activities were highly sensitive to the absorption ratio from shell to core (ARSC), which was defined as the absorption ratio of the CdS shell to the CdSe core, indicating that the signal of CPL increased as the ARSC decreased. The chiral interactions between the DRs and cysteine molecules were regarded to be the key point in generating CPL, however, the exact induction mechanism of CPL still remains to be explored. With the help of a study about the molar ratio of DRs to the chiral cysteine, it was found that an excess of cysteine molecules in an aqueous solution suppresses the CPL activities, which provides a feasible method for changing the induced chirality for potential and important applications. Then, as shown in Figure 3B, Cheng and co-workers also presented CPL-active CdSe/CdS NCs with several morphologies such as nanoflowers, tadpoles with one to three tails, and dot/rods Which induced by surface ligands chirality.[56] The obtained CdSe/CdS NCs nanostructures with different geometrical characteristics exhibited circularly polarized light in multiple wavelengths. The CPL behavior of these samples could be enhanced with the CdS shell thickness thins, however, that is proportional to the photoluminescence quantum efficiency. The effective number of cysteine molecules increases as the aspect ratio increases, resulting in enhancing interactions between the surface chiral ligands and CdSe cores, which gives rise to stronger CPL intensity. Additionally, the quantum efficiency of different NCs gradually decreases as the thickness of the shell increases due to a mismatch between the defects and the shell lattice. These findings provide insights into the rational design of tunable CPL-active CdSe/CdS nanostructures.

In addition, the CPL-active CdSe/CdS core-shell NCs can be obtained by surface chiral ligand-induced. Endowing perovskite with chiroptical properties through chiral ligand exchange starts a new research field of CPL materials. Duan and co-workers have reported the CPL-active $CsPbBr_3$ NCs modified by chiral ligand α-octylamine, and the chirality of $CsPbBr_3$ NCs was attributed to the surface induction from chiral capping ligands (Figure 3C).[57] The α-octylamine capped $CsPbBr_3$ NCs with great photoluminescence ability showed mirror-imaged CPL signal with low scattering and strong chiral properties. The $|g_{lum}|$ values at the maximum emission wavelength of *S*- and *R*-Pero-NCs in hexane were calculated to be 1.0×10^{-3} and 6.5×10^{-4}, respectively. It is worth noting that, compared to 2.8×10^{-3} and 4.5×10^{-3} obtained through one-photon absorption process, the $|g_{lum}|$ value of *S*- and *R*-Pero-NCs in poly(methylmethacrylate) (PMMA) films could be amplified up to 6.5×10^{-3} and 7.0×10^{-3} via two-photon-absorption-based upconverted CPL (TP-UCPL) process. That is similar to the reported triplet-triplet annihilation-based upconverted CPL system. To some extent, the TP-UCPL process could amplify the luminescence dissymmetry factor more greatly than the normal process, which provides a new mechanism to achieve CPL with a

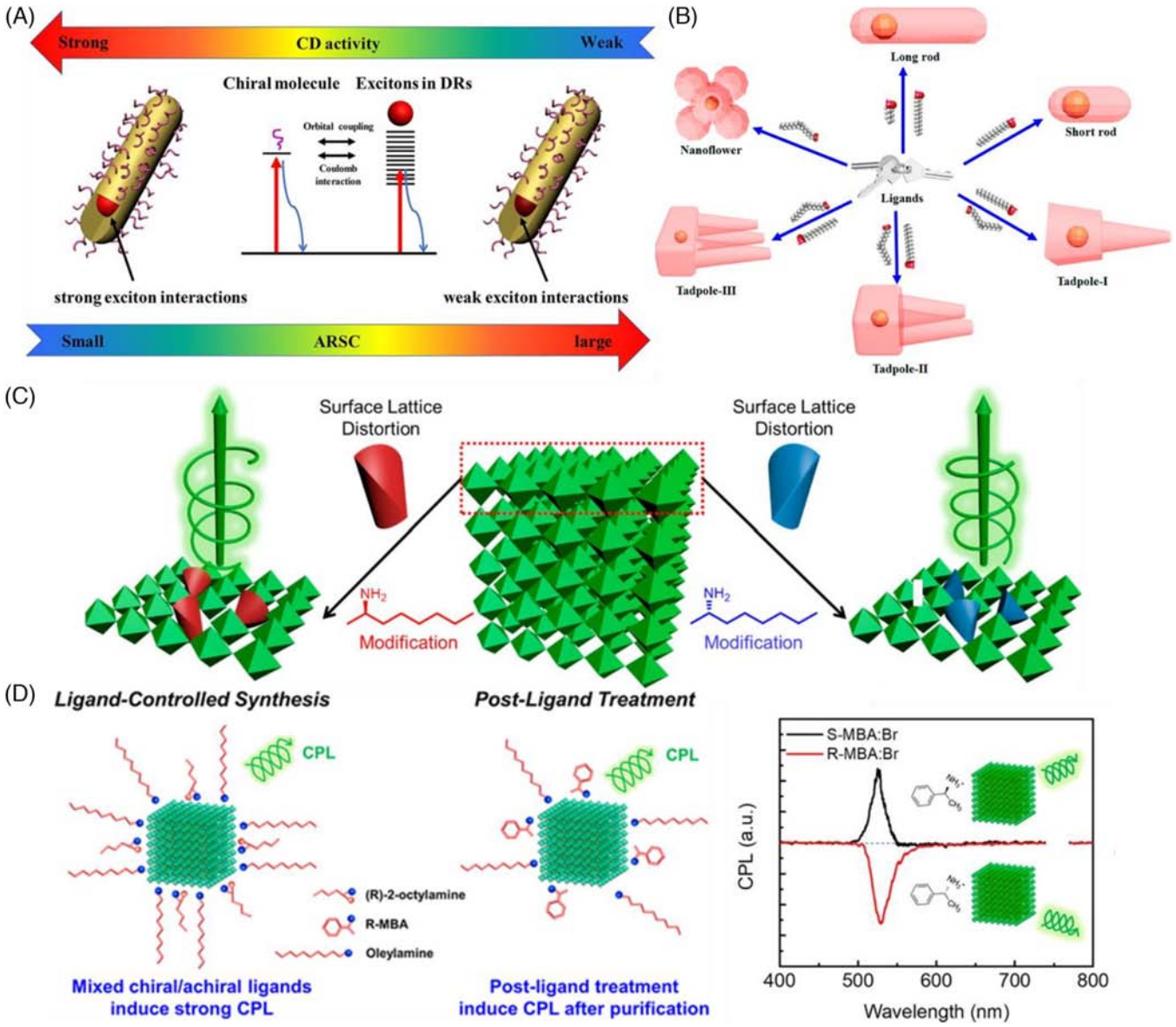

FIGURE 3 Ligand-induced chirality-based circularly polarized luminescence (CPL)-active inorganic nanomaterials. (A). The transitions and interactions between the semiconductor nanocrystal (NC) and the chiral molecule are illustrated, and its relationship with the circular dichroism (CD) activity is followed by the absorption ratio from shell to core (ARSC) effect. The curved blue arrows and red vertical arrows represent relaxations and excitation transitions, respectively. Reproduced with permission: Copyright 2018, American Chemical Society.[55] (B) Mechanism of various anisotropic shapes by ligand-induced such as nanoflowers, tadpoles with one to three tails, and dot/rods. Reproduced with permission: Copyright 2020, American Chemical Society.[56] (C) Schematic illustration of the chiral origin of chiral $CsPbBr_3$ perovskite. Reproduced with permission: Copyright 2019, American Chemical Society.[57] (D) Left: Schematic illustrations of $FAPbBr_3$ NCs with (*R*)-2-octylamine through ligand-controlled synthesis and $FAPbBr_3$ NCs with *R*-/*S*-MBA:Br by post-synthetic ligand treatment. Bottom: CPL spectra of ligand-treated $FAPbBr_3$ NCs with *R*-/*S*-MBA:Br (right). Reproduced with permission: Copyright 2020, American Chemical Society[58]

larger dissymmetry factor. Additionally, the CPL responsiveness colloidal formamidinium lead bromide chiral ($FAPbBr_3$) NCs with high g_{lum} (6.8×10^{-2}) was successfully achieved by Luther and co-workers (Figure 3D).[58] First, the $FAPbBr_3$ NCs were fabricated by replacing some typical ligands (oleylamine) binding on the NCs surfaces with short chiral ligands ((*R*)-2-octylamine), which shows strong CPL with a high g_{lum} (6.8×10^{-2}). The amount of chiral ligands affects the size, NCs photophysics, and surface chemistry. As the concentration of (*R*)-2-octylamine decreases from 100% to 25%, $FAPbBr_3$ NCs show blue-shifted fluorescence spectroscopy as well as the intensified CPL, while the g_{lum} increases from 2.8×10^{-2} to 6.8×10^{-2}, which is due to the mall NCs. The high surface-to-volume ratio of NCs provides the opportunity to let more surface chiral ligands attach to the surface, therefore, the distance between electronic states in the core NCs and surface chiral ligands becomes shorter. This will induce the influence caused by chiral ligands such as surface defects on the wave function of electron-hole in NCs, chiral ligand-induced surface lattice distortion, and electronic coupling. Using a post-synthetic ligand treatment procedure, the researchers attached chiral (*R*-/*S*-) methylbenzylammonium bromide to the surface of purified NCs. The obtained samples emitted strong CPL with an average g_{lum} of $\pm 1.18 \times 10^{-2}$, which is important for employing perovskite NCs in spintronic or optoelectronic devices.

3.3 | Chiral assemblies endow inorganic nanomaterials with CPL activities

The introduction of the "chiral assembly" concept provides a new viewpoint in achieving the CPL-active inorganic nanomaterials. Chiral assembly indicated the capacity of the chirality transfer from the chiral template to the achiral inorganic nanomaterials. This kind of approach, as an intriguing method for fabricating CPL-active inorganic nanomaterials, has been widely demonstrated. Generally, the guest of the achiral inorganic nanomaterials could be incorporated into an assembled chiral host. Thus, the inorganic CPL-active system by "luminescent guest-chiral host" strategy has been proposed. The achiral inorganic fluorescent materials are incorporated into the chiral host by co-assembly, subsequently, endowing the achiral molecule with CPL activity. For example, the luminescent components could be achiral inorganic metal clusters (Ag) or semiconductor QDs (CdSe, ZnS). The chiral hosts are often liquid crystals, cellulose NCs, supramolecular assemblies or gels, and so forth. Based on such a feasible approach, various CPL-active inorganic nanomaterials were reported. In practice, there are many advanced investigations related to CPL-active inorganic nanomaterials obtained by the chiral assembly.[36,59–64] For example, Oda and Sagawa et al., reported that the inorganic silica showing left (or right) handed nanohelices were used as chiral templates to generate CPL properties of $CsPbBr_3$ NCs.[65] Kawai et al., constructed the nanofiber-based chiral silica systems with CPL activity to endow inorganic luminescent achiral guests such as lead-halide type perovskites with CPL feature.[66] Zhao's group recently constructed a spirocyclic nonnuclear silver cluster compound by sharing the vertices of the two in-situ generated heteroaryl diide-centered metal rings. The core-peripheral type clusters form micrometer-long nanofibers along with strong CPL ($g_{lum} = 0.16$) under the different assembly processes.[67] Yao and co-workers reported phosphine-copper iodide hybrid clusters with robust chirality and their layered assemblies in hexagonal platelet-shaped microcrystals states for amplified CPL with high g_{lum} value (9.5×10^{-3}).[68] Zhao and co-workers fabricated a pair of biocompatible and robust chiral enantiomeric alkynyl-protected L/D-Au_{10} $(C_{13}H_{17}O_5)_{10}$ nanoclusters (L/D-AuNCs) having great luminescent circular polarization property ($g_{lum} \approx 3 \times 10^{-3}$), which can serve as radiosensitizers to explore the effect of chirality on radiotherapy, proving the significance of chirality in biomedicine.[69]

Chiral compounds that can be assembled into chiral supramolecule have been utilized in the preparation of CPL-active nanomaterials. Through noncovalent interactions, achiral inorganic nanomaterials can be bound with chiral compounds and co-assembled into helical structures, while chirality would be transformed from the chiral compounds to the inorganic nanomaterials so that they can be endowed with CPL property. In this method, suitable designs of the chiral compounds are vitally important because inorganic nanomaterials need to have ideal interaction with the chiral host and form the ordered structure. Chiral gels are excellent candidates to obtain inorganic CPL materials. We have successfully co-assembled achiral colorful semiconductor QDs with chiral gelators, observing the CPL signal with the g_{lum} up to 10^{-3} (Figure 4A).[70] The QDs used here were capped with achiral 3-mercaptopropionic acid. Electrostatic interaction, as well as hydrogen bonds between the -NH_2 group and 3-mercaptopropionic acid, played major roles in the construction of the assemblies. The emission colors of QDs remained unchanged, while CPL signals were observed within the full-color range. It was mentioned that too long reagent may hinder chiral transfer and further influence CPL property. Furthermore, by changing the ratio of various colorful QDs, the circularly polarized white light emission was successfully achieved for the first time.

Besides, by using perovskite NCs, we have obtained similar systems with CPL properties (Figure 4B).[71] In this work, perovskite NCs were synthesized by a polar-solvent-free approach, and their emission colors varied from blue, green to red with the change of the halide composition of the precursor. Then, amine-containing gel (LGAm/DGAm) was chosen to introduce the chirality. The gelators and perovskite NCs can coassemble to form chiral nanotubes in nonpolar solvents, showing strong mirror-image CPL signals in the full-color range, while their disassembled state kept CPL silent, indicating that supramolecular coassembly played an important role in the induced CPL property. The supramolecular structure was further studied by scanning electron microscopy, TEM, and fluorescent microscopy, which showed that the mixing of perovskite NCs did not destroy the structure of the gels.

Generally, a CPL-active system needs a chiral component, while the development of completely achiral CPL systems remained a challenge. Achiral C_3-symmetric benzene 1,3,5-tricarboxamid including three identical benzoic acid arms (BTABA) could assemble into a chiral structure via symmetry breaking.[72] Figure 5A gives an example for fabricating a CPL material without the help of chiral compounds. Two kinds of inorganic lanthanide upconversion nanoparticles (UCNPs: $NaYF_4$:Yb/Er and $NaYF_4$:Yb/Tm), with surface modified by 1,1-aminoundecanoic acid, were co-assembled with BTABA, forming functional helical assemblies. By applying vortex mixing, BTABA/UCNPs aggregates show a strong and controlled supramolecular chirality. The ultimate co-assemblies exhibited outstanding CPL performance at both emission peaks of each UCNPs due to the chiroptical activities of the chiral templates and the interaction between the luminescent materials and chiral template, and the g_{lum} arrived at 1.2×10^{-2}. Through this method, we can fabricate the CPL materials in totally achiral compounds, which get rid of the complicated synthesis of the chiral enantiomers.

Besides the chiral assemblies and gels, chiral liquid crystals were proven to be an excellent chiral matrix for fabricating CPL-active materials. After embedding chiral dopant into the achiral nematic liquid crystals, induced chiral nematic liquid crystals (N*LCs) can be obtained. N*LCs as a chiral template can incorporate various inorganic nanomaterials to generate CPL performance.[73,74] We have demonstrated the first example of upconverted CPL (UC-CPL) with high g_{lum} (1.1) through the energy transfer process from UCNPs to the $CsPbBr_3$ perovskite NCs (PKNCs) in N*LCs (Figure 5B).[75] In this work, $CsPbBr_3$ PKNCs was acted as the energy acceptors, whose emission spectra were located at the center of the photonic bandgap of N*LCs, while the emission spectra of UCNPs were seated at the edge of the photonic bandgap of N*LCs. In this situation, a larger g_{lum} value was achieved because of the intense reflection in the center

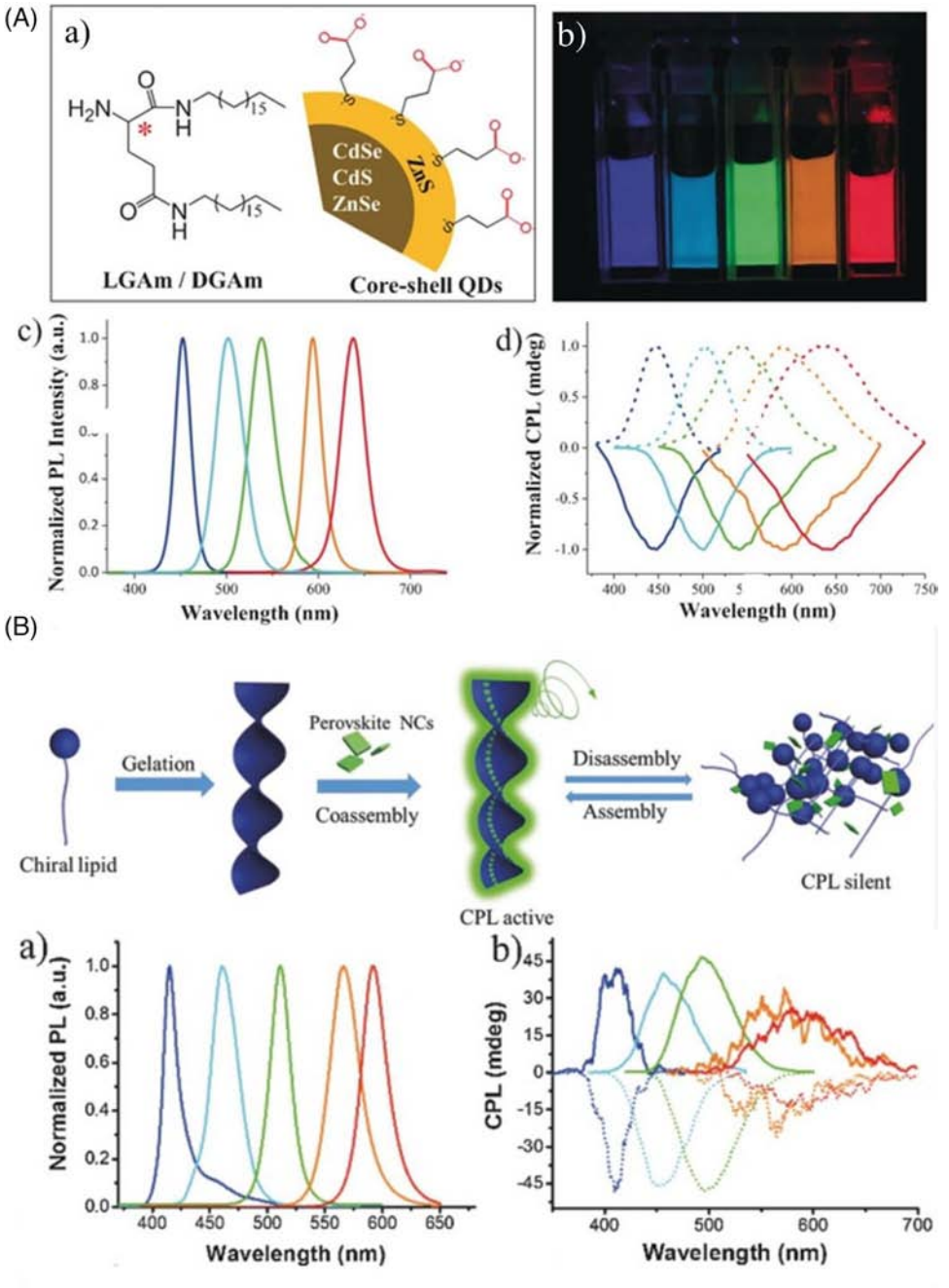

FIGURE 4 Chiral assembly-based circularly polarized luminescence (CPL)-active inorganic nanomaterials. (A) Top: molecular structure of the quantum dots (QDs) and gelators (left) and the picture of various CdSe/ZnS QD doped co-gels (right). Bottom: fluorescence spectra of the corresponding co-gels (left) and mirror-image CPL spectra of the corresponding co-gels (right). Reproduced with permission: Copyright 2017, Wiley-VCH.[70] (B) Top: Illustration of the possible coassembly process of perovskite nanocrystals (NCs) in chiral gels with CPL property in silent or active. Chiral lipid can form gel through the chiral assembly. After adding perovskite NCs, they could form co-gels through coassembly. Bottom: Fluorescence spectra of the corresponding $CsPbX_3$ NCs doped chiral gelators (left) and mirror-image CPL spectra of the corresponding co-assembly samples (right). Reproduced with permission: Copyright 2018, Wiley-VCH[71]

of the photonic bandgap. On the other hand, the enhanced emission of UCNPs was also obtained deriving from the photonic band edge. As a result, the $CsPbBr_3$ PKNCs could reabsorb the enhanced emission of UCNPs, resulting in enhancing the emission of $CsPbBr_3$ PKNCs. Moreover, when applying the electric field in the system, the emission of UC-CPL and the process of radiative energy transfer could be switched off and recovered to the original state by applying the mechanical force. This cycle could run many times, showing a stable electric field-controlled UC-CPL switching ability. This is the first example of achieving the UC-CPL with a high dissymmetry factor via steering the photonic bandgap.

Cellulose NCs (CNCs) are derived from acid hydrolysis, that have the ability to form the chiral nematic structures through a self-assemble process from a colloidal suspension. It is worth noting that the helical ordering of the CNCs can be preserved after drying to form a chiral solid film.[76,77] More importantly, the solid CNCs photonic films have the ability to reflect circularly polarized light with opposite handedness and transmit circularly polarized light with the same handedness.[78] Therefore, by doping achiral inorganic luminescent materials, such as aggregation-induced emission molecules into the self-assembled chiral CNCs, the CPL signals could be obtained.[79,80] For example, Sun's

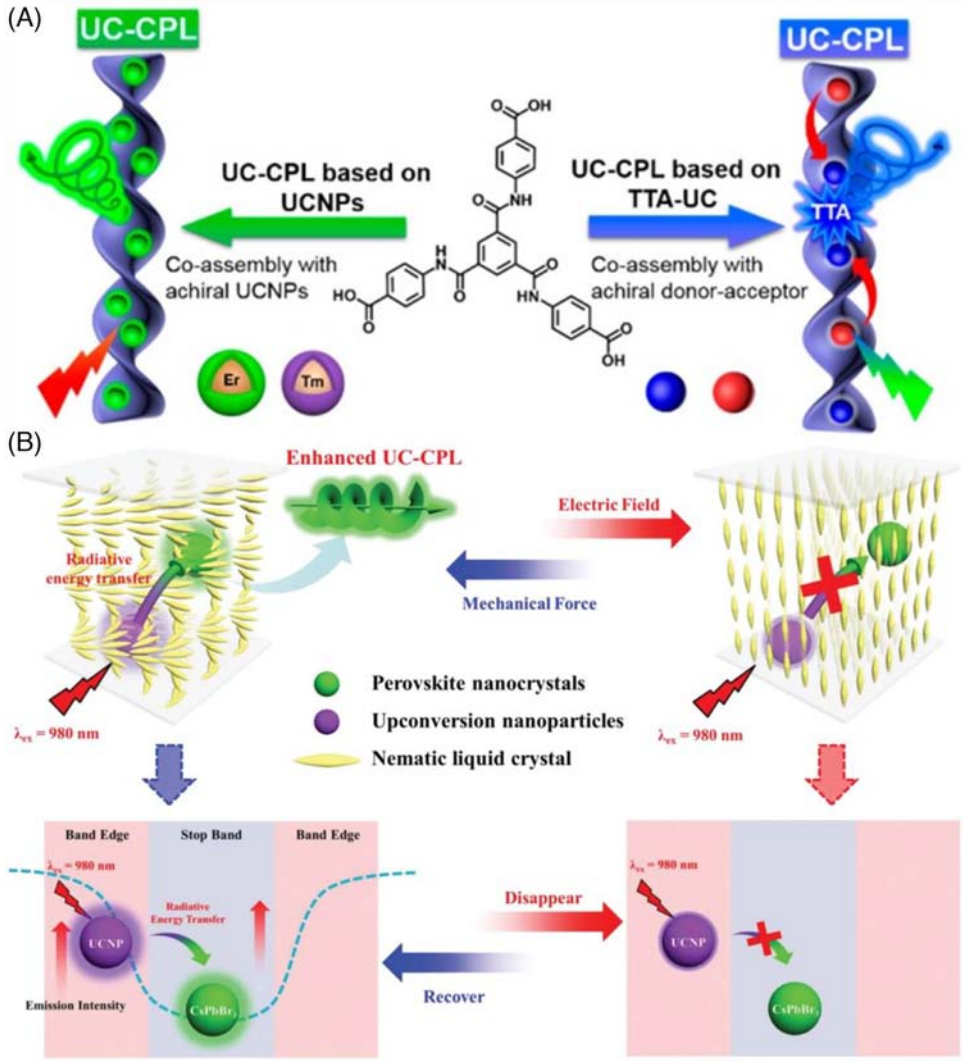

FIGURE 5 (A) Schematic representation of upconverted circularly polarized luminescence (UC-CPL) within achiral systems: symmetry breaking induced supramolecular chirality in the BTABA gel system can be gained during the assembly process. UC-CPL is successfully obtained by adding the inorganic upconversion nanoparticles (UCNPs) or organic donor-acceptor into these chiral supramolecular systems. Reproduced with permission: Copyright 2021, American Chemical Society.[72] (B) Appropriate amounts of UCNPs and $CsPbBr_3$ perovskite NCs (PKNCs) were dropped into the nematic liquid crystals (N*LCs), generating UC-CPL through the radiative energy transfer process. Applying the electric field in the system, the process could be controlled. Reproduced with permission: Copyright 2020, Wiley-VCH[75]

group demonstrated a solid film with circularly polarized luminescent property by doping CdSe/CdS QRs into the self-assembled left-handed helical structure CNCs.[81] The g_{lum} of CPL could be changed by adjusting the relative position between the photonic bandgap and luminescent band: g_{lum} arrived at its maximum value when luminescent band located at the center of the photonic bandgap and gradually decrease when they left away. Liu and co-workers encapsulated semiconductor QDs in CNCs-based left-handed hierarchical photonic films through a co-assembly strategy and obtained analogous g_{lum} values changeable system. These works offer an effective and powerful platform to generate CPL of semiconductor quantum materials.[82]

4 | CPL-BASED PHOTOCHEMICAL AND PHOTOPHYSICAL APPLICATIONS

By and large, the enhancement of chiroptical activity is expected to be acted as the important research direction in inorganic chiral nanostructures. CPL-active inorganic nanomaterials as a new promising field have developed rapidly. Endowing the achiral inorganic nanomaterials with CPL character in respect to their applications in the area of chiroptical detection and sensing, enantioselective photopolymerization, biology-related fields, and chirality-based devices. Since the details about the potential and possible applications of chiral inorganic nanomaterials were well summarized in some great reviews, we would present representative examples of inorganic nanomaterials with CPL property.

Based on recent progress, inorganic nanomaterials with outstanding optoelectronic properties employed as circularly polarized light detectors and sensors have become an emergent research direction. Yuan and co-workers reported that chiral perovskite can distinguish different polarization states of circularly polarized photons with excellent detection performance (Figure 6A).[83] In this work, the chiral quasi-2D perovskite with intrinsic chirality, $[(S)\text{-}\beta\text{-MPA}]_2MAPb_2I_7$ and $[(R)\text{-}\beta\text{-MPA}]2MAPb_2I_7$ SCs, were grown through the method of temperature cooling. The photodetector exhibits notably different photocurrent between left-handed CPL (L-CPL) and right-handed CPL (R-CPL) illumination at 532 nm.

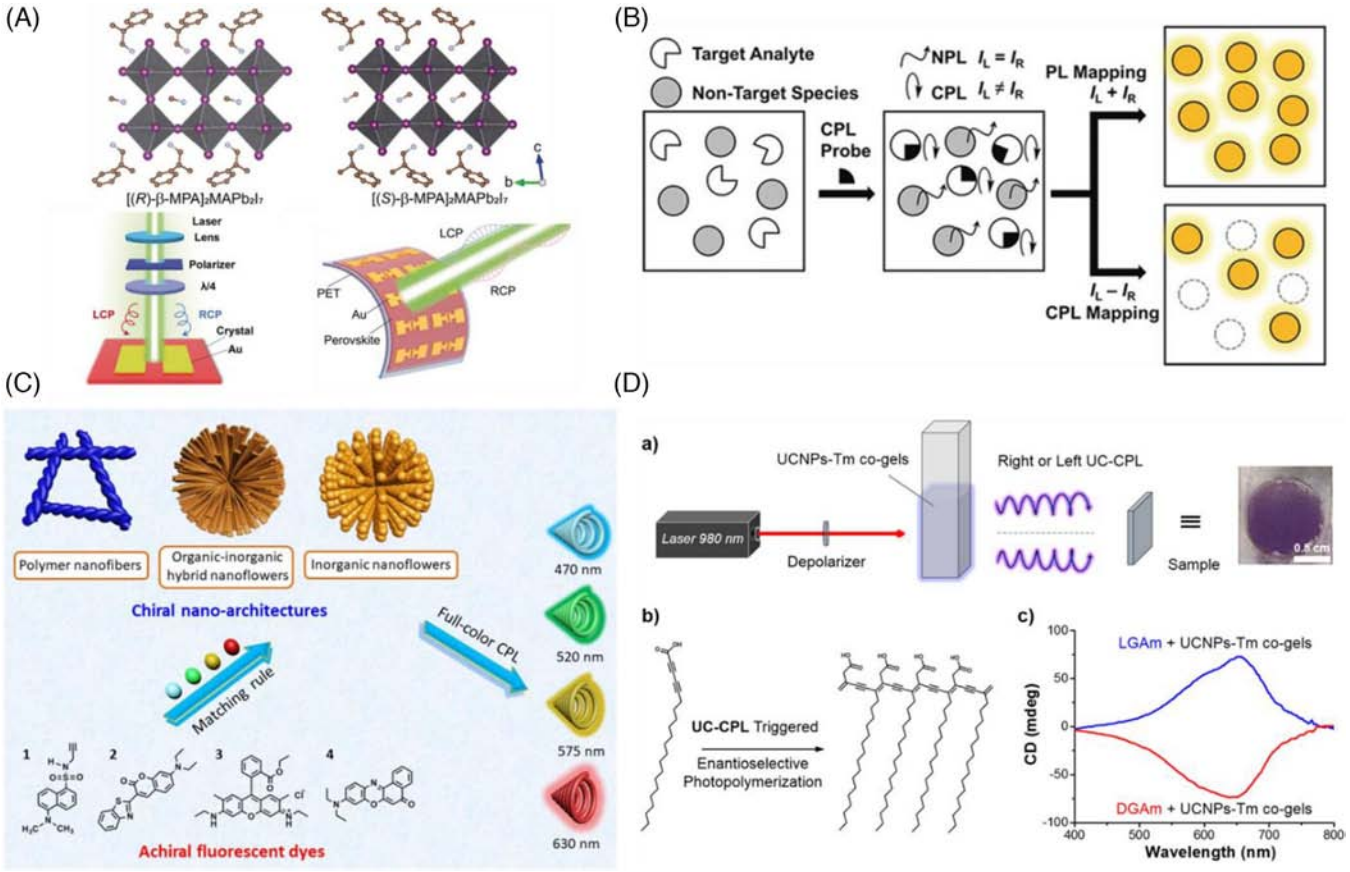

FIGURE 6 Typical applications of inorganic nanomaterials related to circularly polarized luminescence (CPL). (A) Top: Structure of [(S)-b-MPA]$_2$MAPb$_2$I$_7$ and [(R)-b-MPA]$_2$MAPb$_2$I$_7$ single crystals (SCs); Bottom: Illustration of the experimental set-up (left) and the flexible film (right) of the [(R)-b-MPA]$_2$MAPb$_2$I$_7$ SC photodetector under excited by RCP and LCP illumination at 532 nm. Reproduced with permission: Copyright 2020, Wiley-VCH.[83] (B) Illustration of sensor method utilizing the CPL signal as detection output for target recognition. Reproduced with permission: Copyright 2018, Wiley-VCH.[81] (C) Full-color CPL by utilizing CuO (calcinated from CuO/CNC) nanoflowers and CuO/CNC as template coated with achiral organic dyes (1–4). Reproduced with permission: Copyright 2020, American Chemical Society.[85] (D) Illustration of the enantioselective photopolymerization of 2,4-heneicosadiynoic acid (HA) and the circular dichroism (CD) spectra of polydiacetylene (PDA) films after exposure to the UC-CPL emission generated from the upconversion nanoparticles (UCNPs)-Tm doped co-gels. Reproduced with permission: Copyright 2019, American Chemical Society[86]

Right circularly polarized light (RCP) and left circularly polarized light (LCP) photons distinguish a lot, as photocurrent achieved under RCP illumination is much higher than the LCP illumination in the same intensity. Then, based on this chiral quasi-2D perovskite film, they constructed a bendable and flexible CPL photodetector with high responsivity up to 1.1 AW^{-1} and detectivity up to 2.3×10^{11} Jones, which can act as a promising candidate for stable and sensitive CPL photodetectors. Complementary, a new sensor strategy using CPL as a detection output was reported by Yuasa and Kawai's group.[84] Figure 6B presents the sensing method utilizing the CPL signal as a detection output for target recognition. In this case, the chiral probe (R, R)-Im$_2$Py and (S, S)-Im$_2$Py contains two chiral imidazole moieties at the 1,6-positions through ethynyl spacers, which can self-assemble into P or M helicity chiral stacks upon tetrahedral coordination to metal ions such as Zn^{2+}, resulting in triggering strong CPL. This distinct chiroptical switching properties of these cleverly designed probes will allow the construction of innovative sensing systems based on CPL.

Deng and co-workers reported a handed-selective fluorescence filter to formidably transform non-polarized light into CPL (Figure 6C).[85] The as-prepared nanoarchitectures were composed of organic polymer nanofibers (polyacetylene), organic-inorganic hybrid nanoflowers (CuO@CNC), and inorganic nanoflowers (CuO). When fluorescent light of the achiral fluorescence dyes passes through the chiral nanoarchitecture, the emissive light with highly polarized leads to CPL emissions. There is no interaction between fluorescent components and chiral for achieving CPL emission. Thus, a great deal of CPL materials with full-color emission and high g_{lum} factors (-0.025) were prepared. Light-emitting diodes (LEDs) with circularly polarized light (spin-LEDs) properties have a broad prospect in various fields. Kim et al., reported chiral-induced spin selectivity including self-assembly of small chiral molecules in a layered metal halide perovskite NCs to generate spin-polarized carriers and demonstrate a spin-LED that works at room temperature. The spin-LED gets ±2.6% circularly polarized electroluminescence at room temperature.[87]

In addition, we reported the UV light of the UC-CPL generated from the organic-inorganic supramolecular co-assembly system can be utilized to induce the enantioselective photopolymerization of diacetylene derivatives (Figure 6D).[86] Two kinds of achiral lanthanide-doped upconversion nanoparticles (UCNPs), NaYF$_4$:Yb/Er (UCNPs-Er) and NaYF$_4$:Yb/Tm (UCNPs-Tm), were helically incorporated into chiral nanotubes derived from chiral gelators LGAm. The UCNPs can absorb more than two low-energy photons and convert the near-infrared (NIR) light into high-energy

light (anti-Stokes shift).In this case, UC-CPL could be easy to achieve under the excitation by a nonpolarized 980 nm laser. Interestingly, mirror-image UC-CPL signals were obtained between 300 nm (UV light) and 850 nm (near-infrared light). To observe the UC-CPL, in the assembled state, the chirality of gelator with the inherent chirality had a capability transferring to the UCNPs. In this case, there was no UC-CPL signal can be observed from the assembled state of the chiral gelator/UCNP mixtures. These results indicate that the self-assembly process is an ideal method for chirality transfer since the obtained chiral nanotube can encapsulate UCNPs into its hollow structure. More importantly, the UC-CPL produced from the co-gels could directly irradiate on the 2,4-heneicosadiynoic acid (HA) film, resulting in the color change of HA film to blue. This implies that the photopolymerization of HA occurred. The polydiacetylene (PDA) showed mirror-image CD spectra, which were consistent with the handedness of circularly polarized light. This work provided a novel idea to develop CPL materials with a diversity of applications in the future. Kuang and Xu et al., reported co-gels (L- or D-[Gel+FeS_2]) with CPL g-factor value of $\pm$0.06 via chiral FeS_2 QDs co-assembled with gelators N-(9-fluorenylmethoxycarbonyl)-protected glutamic acid and chiral lysine. More significantly, because of the CPL-induced electron transfer, the diameter and helical pitch of the co-gels was tuned by illumination with CPL. This research provides valuable insight into the design and development of chiroptical devices with widespread functions and applications.[88]

5 | CONCLUSIONS AND OUTLOOK

The development of CPL-active inorganic nanomaterials has been experienced vigorous growth, which is mainly focused on metals and semiconductors such as QDs and perovskites. Herein, we provide a summary of the progress in CPL-active inorganic nanomaterials including the origination of the chirality and some potential applications. According to the chirality generation mechanism, chirality in the inorganic nanomaterials with CPL activity can be acquired from three mechanisms: intrinsic chirality, ligand-induced chirality, and chiral assembly. In terms of CPL-active inorganic nanostructure resulting from intrinsic chirality and ligand-induced chirality. It is worth noting that they still have broad progressing room so that researches are still necessary to explore the issues on chiral synthesis, chiral ligand-core interactions, chiral light-matter interactions, and quantum-mechanics theories. It is expected to trigger experiments on innovating the design of materials, stimulating researchers to reappraise the root of electromagnetic response between chiral matters and light and to find new opportunities and challenges in new fields. Now, by introducing chirality to the fluorescent inorganic nanomaterials by flexible self-assembly approach, CPL-active inorganic nanomaterials have developed rapidly. The method without a tediously long-time synthesis process broadens the material categories, enabling the design of systematic with uncomplicated mechanism and fabrication of various CPL inorganic nanomaterials. Moreover, chiral-assembly as a flexible approach is not only useful for inorganic systems but also for organic systems, widening the category of CPL-active materials, which will proceed with a new research field. Although many researchers have made great progress for the CPL-active chiral inorganic nanostructure exploration, further effort should be made to broaden its applications in information storage, spintronics, biomarkers, and three-dimensional display devices.

However, the research field of CPL-active inorganic materials still has unsolved issues that need to be further studied. First, the current CPL spectrometer (JASCO-300) covers only a short wavelength region (visible area), NIR excitation and detection would be even more attractive considering tremendous biological and optoelectronic applications at NIR or microwave bands. One possible strategy, for now, may be the development of chiral UCNPs, but this needs photophysics expertise for instrument modifications, for example, light source setup, therefore only a few groups mentioned above are capable of such task for the moment. Accordingly, a future update on the CPL instrument to longer wavelength excitation and detection would be anticipated. Subsequently, CPL measurements may easily suffer from artifacts generated by linear phenomena such as linear dichroism and birefringence, even though sophisticated skills for instrument alignment and sample preparation may improve the situation. Finally, the CPL technique may be inherently limited to chiral luminophores that are strongly luminescent due to the presence of allowed transitions or have a sufficient time between excitation and emission to completely scramble any orientational distribution created by the excitation beam (See Section 2 for details). This suggests that researchers should keep in mind the natural properties of tested chiral inorganic materials (Photoluminescence properties, dimensions, homogeneity, orientation, etc.) as well as CPL setups to obtain as reliable reports as possible.

In sum, we wish the present work will help motivate and enrich the research area of CPL-active inorganic nanomaterials, forcing further development in advanced chiroptical materials as well as bringing new insights for the audience in the realm of stereo-synthesis, chiroptics, optoelectronics, and biological theragnostics.

ACKNOWLEDGEMENTS

This work was supported by the National Natural Science Foundation of China (21802027, 21905065, and 91856115), the Strategic Priority Research Program of the Chinese Academy of Sciences (XDB36000000), and the Ministry of Science and Technology of the People's Republic of China (2017YFA0206600).

CONFLICT OF INTEREST

The authors declare no conflict of interest.

ETHICS STATEMENT

The authors confirm that the data supporting the findings of this study are available within the article.

DATA AVAILABILITY STATEMENT

The authors confirm that the data supporting the findings of this study are available within the article.

ORCID

Rui Chen https://orcid.org/0000-0002-0445-7847
Pengfei Duan https://orcid.org/0000-0002-5971-7546

REFERENCES

1. Y. Wang, J. Xu, Y. Wang, H. Chen, *Chem. Soc. Rev.* **2013**, *42*, 2930.
2. D. J. Kissick, D. Wanapun, G. J. Simpson, *Annu. Rev. Anal. Chem.* **2011**, *4*, 419.
3. D. -Y. Du, L. -K. Yan, Z. -M. Su, S. -L. Li, Y. -Q. Lan, E. -B. Wang, *Coord. Chem. Rev.* **2013**, *257*, 702.
4. Y. Liu, W. Xuan, Y. Cui, *Adv. Mater.* **2010**, *22*, 4112.
5. N. Berova, P. L. Polavarapu, K. Nakanishi, R. W. Woody, *Comprehensive Chiroptical Spectroscopy*, 1st ed., John Wiley & Sons, Hoboken, NJ **2011**.
6. D. M. Rogers, S. B. Jasim, N. T. Dyer, F. Auvray, M. Réfrégiers, J. D. J. C. Hirst, *Chem* **2019**, *5*, 2751.
7. G. Longhi, E. Castiglioni, J. Koshoubu, G. Mazzeo, S. Abbate, *Chirality* **2016**, *28*, 696.
8. D. -W. Zhang, M. Li, C. -F. Chen, *Chem. Soc. Rev.* **2020**, *49*, 1331.
9. M. Li, S. -H. Li, D. Zhang, M. Cai, L. Duan, M. -K. Fung, C. -F. Chen, *Angew. Chem. Int. Ed.* **2018**, *57*, 2889.
10. J. Han, S. Guo, H. Lu, S. Liu, Q. Zhao, W. Huang, *Adv. Opt. Mater.* **2018**, *6*, 1800538.
11. Y. Kim, B. Yeom, O. Arteaga, S. J. Yoo, S. -G. Lee, J. -G. Kim, N. A. Kotov, *Nat. Mater.* **2016**, *15*, 461.
12. M. C. Heffern, L. M. Matosziuk, T. J. Meade, *Chem. Rev.* **2014**, *114*, 4496.
13. R. Carr, N. H. Evans, D. Parker, *Chem. Soc. Rev.* **2012**, *41*, 7673.
14. Y. H. Xia, Y. L. Zhou, Z. Y. Tang, *Nanoscale* **2011**, *3*, 1374.
15. L. Xiao, T. An, L. Wang, X. Xu, H. J. N. T. Sun, *Nano Today* **2020**, *30*, 100824.
16. W. Ma, L. Xu, A. F. de Moura, X. Wu, H. Kuang, C. Xu, N. A. Kotov, *Chem. Rev.* **2017**, *117*, 8041.
17. A. Visheratina, N. A. J. C. C. Kotov, *CCS Chem.* **2020**, *2*, 583.
18. X. Gao, B. Han, X. Yang, Z. Tang, *J. Am. Chem. Soc.* **2019**, *141*, 13700.
19. K. Konishi, M. Nomura, N. Kumagai, S. Iwamoto, Y. Arakawa, M. Kuwata-Gonokami, *Phys. Rev. Lett.* **2011**, *106*, 057402.
20. J. J. Cheng, F. Ge, C. Zhang, Y. Kuai, P. H. Hou, Y. F. Xiang, D. G. Zhang, L. Z. Qiu, Q. J. Zhang, G. Zou, *J. Mater. Chem. C* **2020**, *8*, 9271.
21. S. Ma, J. Ahn, J. Moon, *Adv. Mater.* **2021**, *33*, 2005760.
22. D. Li, X. T. Liu, W. T. Wu, Y. Peng, S. G. Zhao, L. N. Li, M. C. Hong, J. H. Luo, *Angew. Chem. Int. Ed.* **2021**, *60*, 8415.
23. P. Chen, T. W. Lo, Y. Fan, S. Wang, H. Huang, D. Lei, *Adv. Opt. Mater.* **2020**, *8*, 1901233.
24. Y. Li, X. Wang, J. Miao, J. Li, X. Zhu, R. Chen, Z. Tang, R. Pan, T. He, J. Cheng, *Adv. Mater.* **2020**, *32*, 1905585.
25. M. -M. Zhang, K. Li, S. -Q. Zang, *Adv. Opt. Mater.* **2020**, *8*, 1902152.
26. X. Zhao, S. -Q. Zang, X. Chen, *Chem. Soc. Rev.* **2020**, *49*, 2481.
27. A. Ben-Moshe, B. M. Maoz, A. O. Govorov, G. Markovich, *Chem. Soc. Rev.* **2013**, *42*, 7028.
28. X. Gao, X. Zhang, K. Deng, B. Han, L. Zhao, M. Wu, L. Shi, J. Lv, Z. Tang, *J. Am. Chem. Soc.* **2017**, *139*, 8734.
29. L. Xu, M. Sun, W. Ma, H. Kuang, C. Xu, *Mater. Today* **2016**, *19*, 595.
30. Y. Sang, J. Han, T. Zhao, P. Duan, M. Liu, *Adv. Mater.* **2020**, *32*, 1900110.
31. J. J. Liu, L. Yang, P. Qin, S. Q. Zhang, K. K. L. Yung, Z. F. Huang, *Adv. Mater.* **2021**, 2005506.
32. T. A. E. Jakschitz, B. M. Rode, *Chem. Soc. Rev.* **2012**, *41*, 5484.
33. L. F. Wang, Z. L. Wang, *Nano Today* **2021**, *37*, 101108.
34. Z. Fan, A. O. Govorov, *Nano Lett.* **2012**, *12*, 3283.
35. J. Cheng, E. H. Hill, Y. Zheng, T. He, Y. Liu, *Mat. Chem. Front.* **2018**, *2*, 662.
36. H. -Y. Wong, W. -S. Lo, K. -H. Yim, G. -L. Law, *Chem* **2019**, *5*, 3058.
37. F. S. Richardson, J. P. Riehl, *Chem. Rev.* **1977**, *77*, 773.
38. L. Arrico, L. Di Bari, F. Zinna, *Chem. Eur. J.* **2021**, *27*, 2920.
39. I. Z. Steinberg, A. Gafni, *Rev. Sci. Instrum.* **1972**, *43*, 409.
40. J. P. Riehl, F. S. Richardson, *Chem. Rev.* **1986**, *86*, 1.
41. A. R. Miandashti, L. K. Khorashad, M. E. Kordesch, A. O. Govorov, H. H. Richardson, *ACS Nano* **2020**, *14*, 4188.
42. U. Hananel, A. Ben-Moshe, D. Tal, G. Markovich, *Adv. Mater.* **2020**, *32*, 1905594.
43. Z. Guo, J. Li, C. Wang, R. Liu, J. Liang, Y. Gao, J. Cheng, W. Zhang, X. Zhu, R. Pan, T. He, *Angew. Chem. Int. Ed.* **2021**, *60*, 8441.
44. M. Naito, K. Iwahori, A. Miura, M. Yamane, I. Yamashita, *Angew. Chem. Int. Ed.* **2010**, *49*, 7006.
45. D. Di Nuzzo, L. Cui, J. L. Greenfield, B. Zhao, R. H. Friend, S. C. J. Meskers, *ACS Nano* **2020**, *14*, 7610.
46. J. Wang, C. Fang, J. Ma, S. Wang, L. Jin, W. Li, D. Li, *ACS Nano* **2019**, *13*, 9473.
47. J. Ma, C. Fang, C. Chen, L. Jin, J. Wang, S. Wang, J. Tang, D. Li, *ACS Nano* **2019**, *13*, 3659.
48. J. -X. Gao, W. -Y. Zhang, Z. -G. Wu, Y. -X. Zheng, D. -W. Fu, *J. Am. Chem. Soc.* **2020**, *142*, 4756.
49. U. Hananel, A. Ben-Moshe, H. Diamant, G. Markovich, *Proc. Natl. Acad. Sci.* **2019**, *116*, 11159.
50. M. V. Mukhina, V. G. Maslov, A. V. Baranov, A. V. Fedorov, A. O. Orlova, F. Purcell-Milton, J. Govan, Y. K. Gun'ko, *Nano Lett.* **2015**, *15*, 2844.
51. J. Li, J. Li, R. Liu, Y. Tu, Y. Li, J. Cheng, T. He, X. Zhu, *Nat. Commun.* **2020**, *11*, 2046.
52. M. P. Moloney, J. Govan, A. Loudon, M. Mukhina, Y. K. Gun'ko, *Nat. Protoc.* **2015**, *10*, 558.
53. V. Kuznetsova, Y. Gromova, M. Martinez-Carmona, F. Purcell-Milton, E. Ushakova, S. Cherevkov, V. Maslov, Y. K. Gun'ko, *Nanophotonics* **2021**, *10*, 797.
54. U. Tohgha, K. K. Deol, A. G. Porter, S. G. Bartko, J. K. Choi, B. M. Leonard, K. Varga, J. Kubelka, G. Muller, M. Balaz, *ACS Nano* **2013**, *7*, 11094.
55. J. Cheng, J. Hao, H. Liu, J. Li, J. Li, X. Zhu, X. Lin, K. Wang, T. He, *ACS Nano* **2018**, *12*, 5341.
56. J. Hao, Y. Li, J. Miao, R. Liu, J. Li, H. Liu, Q. Wang, H. Liu, M.-H. Delville, T. He, K. Wang, X. Zhu, J. Cheng, *ACS Nano* **2020**, *14*, 10346.
57. W. Chen, S. Zhang, M. Zhou, T. Zhao, X. Qin, X. Liu, M. Liu, P. Duan, *J. Phys. Chem. Lett.* **2019**, *10*, 3290.
58. Y. -H. Kim, Y. Zhai, E. A. Gaulding, S. N. Habisreutinger, T. Moot, B. A. Rosales, H. Lu, A. Hazarika, R. Brunecky, L. M. Wheeler, J. J. Berry, M. C. Beard, J. M. Luther, *ACS Nano* **2020**, *14*, 8816.
59. C. -T. Yeung, K. -H. Yim, H. -Y. Wong, R. Pal, W. -S. Lo, S. -C. Yan, M. Y. -M. Wong, D. Yufit, D. E. Smiles, L. J. McCormick, S. J. Teat, D. K. Shuh, W. -T. Wong, G. -L. Law, *Nat. Commun.* **2017**, *8*, 1128.
60. M. Sugimoto, X. -L. Liu, S. Tsunega, E. Nakajima, S. Abe, T. Nakashima, T. Kawai, R. -H. Jin, *Chem. Eur. J.* **2018**, *24*, 6519.
61. J. Yan, W. Fang, J. -Y. Kim, J. Lu, P. Kumar, Z. Mu, X. Wu, X. Mao, N. A. Kotov, *Chem. Mater.* **2020**, *32*, 476.
62. J. -Y. Kim, N. A. Kotov, *Science* **2019**, *365*, 1378.
63. W. Hao, Y. Li, M. Liu, *Adv. Opt. Mater.* **2021**, *9*, 2100452.
64. Y. Wang, K. Wan, F. Pan, X. Zhu, Y. Jiang, H. Wang, Y. Chen, X. Shi, M. Liu, *Angew. Chem. Int. Ed.* **2021**, *60*, 16615.
65. P. Liu, W. Chen, Y. Okazaki, Y. Battie, L. Brocard, M. Decossas, E. Pouget, P. Muller-Buschbaum, B. Kauffmann, S. Pathan, T. Sagawa, R. Oda, *Nano Lett.* **2020**, *20*, 8453.
66. S. Tsunega, R. -H. Jin, T. Nakashima, T. Kawai, *ChemPlusChem* **2020**, *85*, 619.
67. H. Wu, X. He, B. Yang, C. -C. Li, L. Zhao, *Angew. Chem. Int. Ed.* **2021**, *60*, 1535.
68. J. -J. Wang, H. -T. Zhou, J. -N. Yang, L. -Z. Feng, J. -S. Yao, K. -H. Song, M. -M. Zhou, S. Jin, G. Zhang, H. -B. Yao, *J. Am. Chem. Soc.* **2021**, *143*, 10860.
69. T. -T. Jia, B. -J. Li, G. Yang, Y. Hua, J. -Q. Liu, W. Ma, S. -Q. Zang, X. Chen, X. J. N. T. Zhao, *Nano Today* **2021**, *39*, 101222.
70. S. Huo, P. Duan, T. Jiao, Q. Peng, M. Liu, *Angew. Chem. Int. Ed.* **2017**, *56*, 12174.
71. Y. Shi, P. Duan, S. Huo, Y. Li, M. Liu, *Adv. Mater.* **2018**, *30*, 1705011.
72. M. Zhou, Y. Sang, X. Jin, S. Chen, J. Guo, P. Duan, M. Liu, *ACS Nano* **2021**, *15*, 2753.
73. H. Wang, L. Wang, H. Xie, C. Li, S. Guo, M. Wang, C. Zou, D. Yang, H. Yang, *RSC Adv.* **2015**, *5*, 33489.
74. H. K. Bisoyi, Q. Li, *Acc. Chem. Res.* **2014**, *47*, 3184.
75. X. Yang, M. Zhou, Y. Wang, P. Duan, *Adv. Mater.* **2020**, *32*, 2000820.
76. Y. Habibi, L. A. Lucia, O. J. Rojas, *Chem. Rev.* **2010**, *110*, 3479.
77. M. Giese, M. Spengler, *Mol. Syst. Des. Eng.* **2019**, *4*, 29.
78. H. Z. Zheng, W. R. Li, W. Li, X. J. Wang, Z. Y. Tang, S. X. A. Zhang, Y. Xu, *Adv. Mater.* **2018**, *30*, 1705948.
79. J. He, K. Bian, N. Li, G. Piao, *J. Mater. Chem. C* **2019**, *7*, 9278.
80. H. Yu, B. Zhao, J. Guo, K. Pan, J. Deng, *J. Mater. Chem. C* **2020**, *8*, 1459.
81. Y. Shi, Z. Zhou, X. Miao, Y. J. Liu, Q. Fan, K. Wang, D. Luo, X. W. Sun, *J. Mater. Chem. C* **2020**, *8*, 1048.
82. M. Xu, C. Ma, J. Zhou, Y. Liu, X. Wu, S. Luo, W. Li, H. Yu, Y. Wang, Z. Chen, J. Li, S. Liu, *J. Mater. Chem. C* **2019**, *7*, 13794.

83. L. Wang, Y. Xue, M. Cui, Y. Huang, H. Xu, C. Qin, J. Yang, H. Dai, M. Yuan, *Angew. Chem. Int. Ed.* **2020**, *59*, 6442.
84. Y. Imai, Y. Nakano, T. Kawai, J. Yuasa, *Angew. Chem. Int. Ed.* **2018**, *57*, 8973.
85. B. Zhao, H. Yu, K. Pan, Z. A. Tan, J. Deng, *ACS Nano* **2020**, *14*, 3208.
86. X. Jin, Y. Sang, Y. Shi, Y. Li, X. Zhu, P. Duan, M. Liu, *ACS Nano* **2019**, *13*, 2804.
87. Y. H. Kim, Y. X. Zhai, H. P. Lu, X. Pan, C. X. Xiao, E. A. Gaulding, S. P. Harvey, J. J. Berry, Z. V. Vardeny, J. M. Luther, M. C. Beard, *Science* **2021**, *371*, 1129.
88. C. Hao, Y. Gao, D. Wu, S. Li, L. Xu, X. Wu, J. Guo, M. Sun, X. Li, C. Xu, H. Kuang, *Adv. Mater.* **2019**, *31*, 1903200.

AUTHOR BIOGRAPHIES

Dongxue Han obtained her B. Eng. degree in Applied Chemistry from the Liaoning Petrochemical University. In 2017, she enrolled in a Ph.D. course at the Yanshan University and National Center for Nanoscience and Technology, under the joint supervision of Prof. Tifeng Jiao and Pengfei Duan, where she is currently in the third year. Her recent research focuses on chiral liquid crystals, photon upconversion, self-assembled chiral responsive materials, and their circularly polarized luminescence.

Dr. Jiaji Cheng's background spans physical, inorganic, and analytical chemistry, quantum materials, and chiroptics. He received his Ph.D. with distinction at Université de Bordeaux in 2015 focusing on chiral inorganic assemblies and nanophotonics. Afterward, he went to Institut de Chimie de la Matière Condensée de Bordeaux as a postdoc researcher studying hierarchical nanomaterials with chiroptical properties. Then he joined Hubei University as an associate professor in 2019. He has broad, multidisciplinary interests in nanophotonics, chiral plasmonics, non-linear and ultrafast optics in hierarchical chiral nanomaterials.

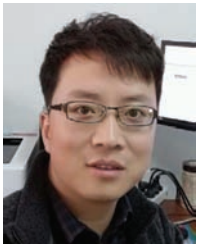

Pengfei Duan received his Ph.D. in chemistry from the Institute of Chemistry, the Chinese Academy of Sciences (China). He worked as a postdoctoral research fellow and assistant professor at Kyushu University (Japan) from 2011 to 2015. Since the end of 2015, he joined the National Center for Nanoscience and Technology (NCNST) as a full professor. His research concerns chiral materials, supramolecular chemistry, photochemistry, and physics.

How to cite this article: D. Han, C. Li, C. Jiang, X. Jin, X. Wang, R. Chen, J. Cheng, P. Duan, *Aggregate* **2022**, *3*, e148. https://doi.org/10.1002/agt2.148